

Publication II

Nikolai B. Kopnin and Juha Voutilainen,
Nonequilibrium charge transport in quantum SINIS structures,
Physical Review B, 75, 174509 (2007).

© (2007) The American Physical Society.
Reprinted with permission.

Nonequilibrium charge transport in quantum SINIS structures

N. B. Kopnin^{1,2} and J. Voutilainen¹

¹*Low Temperature Laboratory, Helsinki University of Technology, P.O. Box 2200, FIN-02015 HUT, Finland*

²*L. D. Landau Institute for Theoretical Physics, 117940 Moscow, Russia*

(Received 19 December 2006; revised manuscript received 6 March 2007; published 14 May 2007)

Charge transport in a high-transmission single-mode long SINIS junction (S stands for superconductor, I is an insulator, and N is a normal metal) is considered in the limit of low bias voltages and low temperatures. The kinetic equation for the quasiparticle distribution on the Andreev levels is derived, taking into account both inelastic relaxation and voltage-driven Landau-Zener transitions between the levels. We show that, for a long junction when the number of levels is large, the Landau-Zener transitions enhance the action of each other and lead to a drastic increase of the dc current far above the critical Josephson current of the junction.

DOI: 10.1103/PhysRevB.75.174509

PACS number(s): 74.45.+c, 74.78.Na, 73.23.-b

I. INTRODUCTION

Weak links consisting of superconducting (S) and normal metal (N) parts separated by insulators (I) are the subject of intensive experimental and theoretical studies. Transport through these systems is determined by several factors, such as transparency of the contacts, specifics of the weak link area, and inelastic relaxation, leading to a series of nonlinear characteristics in the current-voltage (I - V) curve. In stationary regime, numerous configurations have been analyzed (see Ref. 1 for review), revealing the importance of both Andreev² and normal reflection processes taking place in the contact.

When the injection rate of new particles into the junction is greater than the corresponding rate of inelastic relaxation, the nonequilibrium effects are to be taken into account. In realistic junctions with high current density and especially at low temperatures, the inelastic relaxation may become less effective, resulting in a strong nonequilibrium which crucially affects the current transported through the contact. For even a small bias voltage below the energy gap, the oscillating Josephson supercurrent may be accompanied with a non-zero dc component corresponding to the dissipative processes. Nonequilibrium situations in various SINIS-type junctions ranging from a point contact to a ballistic junction with finite length have been studied by many authors; the discussion to some extent has also concerned³⁻⁵ the inelastic relaxation effects. As is well known, the dc component exhibits a subgap structure at bias voltages $eV=|\Delta|/n$ which is associated with multiple Andreev reflections (MAR).^{3,6-8} The quasiparticles trapped in the junction are accelerated by the applied voltage, while, for each cycle of repeated electron-hole reflections at the two NS interfaces, the energy of the particle increases by $2eV$ until the accumulated energy enables it to escape the pair-potential well. This works in a broad voltage range, but becomes more and more complicated when relaxation effects are included or the transparency at the interfaces differs from unity. The low-voltage MAR process for $eV \ll \Delta$ in a ballistic contact is equivalent to the spectral flow along the Andreev energy levels⁹ where the phase difference ϕ adiabatically depends on time $\phi = 2eVt/\hbar + \phi_0$. However, for a nonideal transparency, the energy levels are separated from each other by minigaps (see

Sec. II) which suppress the transitions from one level to the next thus cutting the spectral flow off. As a result, for very low voltages, the dc current is small for contacts with any realistic transparency $\mathcal{T} \neq 1$.

The interlevel transitions can take place by means of Landau-Zener (LZ) tunneling near the avoided crossings of the Andreev levels; they restore the spectral flow and give rise to a finite dissipative current. The LZ processes are more simple in short junctions (point contacts) where only two Andreev states corresponding to particles traveling in opposite directions exist; these levels have only one minigap at the phase difference $\phi = \pi$. Effects of LZ tunneling on the transport properties of quantum point contacts have been studied in Refs. 4, 5, and 10; the dc current was found to have an exponential dependence on voltage in the low-voltage limit.

For junctions where the center island has a length d longer than the superconducting coherence length ξ , the number of levels is proportional to the ratio d/ξ and can, thus, become large. If the transparency is not exactly unity, these levels are separated by minigaps at $\phi = \pi k$, where k is an integer. In practice, such SINIS structures can be made of a carbon nanotube or semiconductor nanowire placed between two superconductors as in Refs. 11 and 12. In Ref. 13 this type of junctions was suggested as a realization of a quantum charge pump where the minigaps were manipulated by the gate voltage being sequentially closed in resonance with the Josephson frequency. In the present paper, we consider the low-temperature charge transport in these junctions and calculate the I - V curve for constant bias and gate voltages. We derive the effective kinetic equation for the quasiparticle distribution on the Andreev levels, taking into account both the inelastic relaxation on each level and the LZ transitions between the neighboring levels, and demonstrate that the voltage-driven LZ transitions from one level to the next enhance the action of each other and lead to a drastic increase of the dc as the transition probability grows with the applied voltage.

We begin with a brief description of the spectral properties of double-barrier SINIS structures in Sec. II. In Sec. III we derive the kinetic equation that determines the distribution function on the Andreev levels in the presence of LZ transitions and inelastic relaxation. In Secs. IV and V we calculate the current and discuss the results.

II. MODEL

We consider a quantum SINIS contact consisting of two superconducting leads connected by a normal conductor that has a single conducting mode. The insulating barriers have a high transparency such that the contact is nearly ballistic. In this section, we briefly summarize the spectral properties of SINIS contacts which are important for the transport characteristics. It is well known that the supercurrent flowing through such contact is determined by the Andreev states formed in the normal conductor and extended into the superconducting leads. The states can be described by the Bogoliubov-deGennes equations,

$$\left[-\frac{\hbar^2}{2m} \frac{d^2}{dx^2} - E_F + U(x) \right] \hat{\sigma}_z \hat{\psi} + \hat{H} \hat{\psi} = \epsilon \hat{\psi}, \quad (1)$$

where $\hat{\sigma}_z$ is the Pauli matrix in Nambu space, and

$$\hat{\psi} = \begin{pmatrix} u \\ v \end{pmatrix}, \quad \hat{H} = \begin{pmatrix} 0 & \Delta \\ \Delta^* & 0 \end{pmatrix}.$$

The superconducting gap is $\Delta = |\Delta| e^{\pm i\phi/2}$ for $x > d/2$ and $x < -d/2$, respectively, while $\Delta = 0$ for $-d/2 < x < d/2$. For simplicity, we model the normal reflections at the interfaces as being produced by δ -function barriers $U(x) = I\delta(x-d/2) + I\delta(x+d/2)$ assuming that the quasiparticle velocity in the superconducting leads is the same as in the normal conductor.

In the normal region, the particle, $e^{\pm iq_x x}$, and hole, $e^{\mp iq_x x}$, waves have amplitudes u^\pm and v^\mp , respectively. The upper or lower signs refer to the waves propagating to the right $\hat{\psi}^> = (u^+, v^-)$ or to the left $\hat{\psi}^< = (u^-, v^+)$. The particle (hole) momentum is $q_\pm = k_x \pm \epsilon/\hbar v_x$, where v_x is the quasiparticle velocity of the mode and $k_x = mv_x/\hbar$. Scattering at the right and left barriers couples the amplitudes of incident and reflected waves,¹⁴

$$\hat{\psi}_R^< = \hat{S}^R \hat{\psi}_R^>, \quad \hat{\psi}_L^> = \hat{S}^L \hat{\psi}_L^<, \quad \hat{S} = \begin{pmatrix} S_N e^{i\delta} & S_A e^{i\chi} \\ S_A e^{-i\chi} & S_N e^{-i\delta} \end{pmatrix}. \quad (2)$$

The scattering matrices for the right and left barriers are $\hat{S}^R = \hat{S}(\chi_R)$ and $\hat{S}^L = \hat{S}(\chi_L)$, respectively, where $\chi_L = -\phi/2$ while $\chi_R = \phi/2$. The scattering matrices are unitary $\hat{S}^\dagger \hat{S} = 1$ because of conservation of the quasiparticle flux. Components of the \hat{S} matrix for δ -like barriers and energies $|\epsilon| < |\Delta|$ are⁶

$$S_N = -\frac{(U^2 - V^2)Z\sqrt{Z^2 + 1}}{U^2 + (U^2 - V^2)Z^2}, \quad S_A = \frac{UV}{U^2 + (U^2 - V^2)Z^2}.$$

Here, $Z = ml/\hbar^2 k_x$ is the barrier strength and $U = 2^{-1/2}(1 + i\sqrt{|\Delta|^2 - \epsilon^2}/\epsilon)^{1/2}$, $V = U^*$. The scattering phase δ is introduced through $\cot \delta = Z$. Applying the scattering conditions at both ends of the normal region, one can derive a compact equation for the spectrum of a SINIS contact,¹³

$$|S_N|^2 \sin^2 \alpha' + |S_A|^2 \cos^2(\phi/2) = \sin^2(\beta + \gamma). \quad (3)$$

Here, $\alpha = k_x d$, $\alpha' = \alpha + \delta$, and $\beta = ed/\hbar v_x$. The phase γ is defined as $S_N = e^{i\gamma}|S_N|$. For short contacts $d \ll \hbar v_x/|\Delta|$, the spectrum has two branches varying from $\epsilon = \pm|\Delta|$ at $\phi = 0$ and

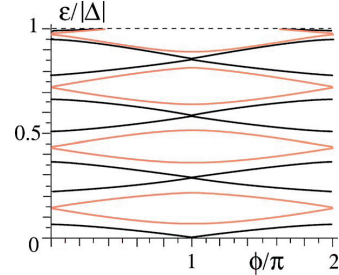


FIG. 1. (Color online) Examples of the spectra [Eq. (3)] for a long SINIS contact with $Z=0.5$ and $|\Delta|d/\hbar v = 10$. Dark (black online) lines: resonance $\sin \alpha' = 0$, the gaps disappear for $\phi = \pi + 2\pi k$; light (red online) lines: antiresonance $\cos \alpha' = 0$, the gaps disappear for $\phi = 2\pi k$.

separated from each other by minigaps at $\phi = \pi + 2\pi k$. The energy spectra of SINIS contacts in various limits have been extensively studied by many authors.¹⁵

In what follows, we focus on long contacts, $d \gg \hbar v_x/|\Delta|$, which have a large number of levels $N \sim d|\Delta|/\hbar v_x$. These levels split off from the states with $\epsilon = \pm|\Delta|$ and fill the energy interval $-|\Delta| < \epsilon < |\Delta|$ with spacings of the order of $\hbar v_x/d$. Examples of the spectra are shown in Fig. 1. Each level is a function of the phase difference ϕ ; its range of variation is of the order of the interlevel spacing. The levels approach each other more closely at $\phi = \pi k$ where they are separated by minigaps. All minigaps at $\phi = \pi(1+2k)$ disappear for the resonance condition, $\sin \alpha' = 0$. Similarly, all minigaps at $\phi = 2\pi k$ disappear for antiresonance, $|\sin \alpha'| = 1$. This follows from Eq. (3) due to unitarity $|S_N|^2 + |S_A|^2 = 1$. The low-energy levels, $\epsilon_l \ll |\Delta|$, $\gamma \ll 1$, have the form

$$\epsilon_l = \pm \epsilon_0 + \pi \hbar v_x l/d, \quad (4)$$

where

$$\epsilon_0 = \frac{\hbar v_x}{d} \arcsin \sqrt{\mathcal{T}^2 \cos^2 \frac{\phi}{2} + (1 - \mathcal{T}^2) \sin^2 \alpha'}, \quad (5)$$

l is an integer, and $\mathcal{T} = (1 + 2Z^2)^{-1}$ is the transmission coefficient of the contact. The energy gaps at $\phi = \pi(1+2k)$ are all equal,

$$\delta \epsilon_\pi = (2\hbar v_x/d) \arcsin(|\sin \alpha'| \sqrt{1 - \mathcal{T}^2}).$$

The gaps $\delta \epsilon_{2\pi}$ at $\phi = 2\pi k$ are given by the same expression where $|\sin \alpha'|$ is replaced with $|\cos \alpha'|$. For a transparent contact, $\mathcal{T} = 1$, all minigaps disappear.

III. KINETIC EQUATION

If a bias voltage V is applied across the superconducting leads, the current through the contact has both ac and dc components. For low voltages, eV much smaller than Δ , the dc component is small for contacts with any transparency $\mathcal{T} \neq 1$. This is due to the presence of minigaps discussed in the previous section. In long contacts, the minigaps exist at $\phi = \pi k$ and suppress the transitions between the levels, thus

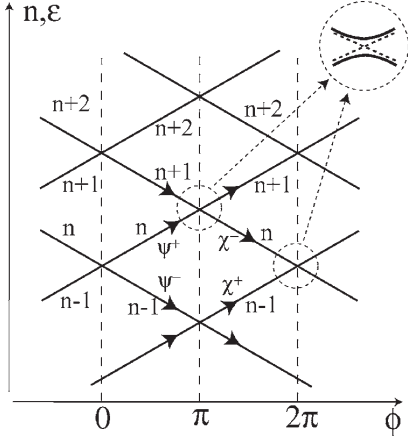


FIG. 2. Scheme of the energy levels as functions of ϕ . The arrows show the direction of the spectral flow. Shown enlarged are avoided crossings of levels at $\phi=\pi k$.

preserving the equilibrium distribution of excitations. As a result, the current through the contact is simply the equilibrium supercurrent with the phase difference ϕ adiabatically depending on time, $\phi=\omega_J t+\phi_0$, where $\omega_J=2eV/\hbar$ is the Josephson frequency. The dc component should thus vanish. However, the time dependence of the phase induces the LZ transitions between the levels near the avoided crossing points at $\phi=\pi k$ which produce deviation from equilibrium. Since the transparency of the contact is of the order of unity, $\mathcal{T}\sim 1$, particles with $|\epsilon|>|\Delta|$ have enough time to escape from the double-barrier region and to relax in the continuum. Particles at the continuum edges with energies $\epsilon=\pm|\Delta|$, which are in equilibrium with the heat bath, are captured on the outermost Andreev levels when the latter split off from the continuum as the phase varies in time. Next, these particles are excited to the neighboring levels due to the interlevel transitions. Relaxation of thus created nonequilibrium distribution gives rise to a finite dc current.

In this section we derive the effective kinetic equation that describes the distribution function on the Andreev levels, taking into account both the inelastic relaxation on each level and the LZ transitions between the neighboring levels. We assume that the LZ transitions take place only near the avoided crossings at $\phi=\pi k$. This can be realized if two conditions are fulfilled. First, the minigaps $\delta\epsilon_\pi$ and $\delta\epsilon_{2\pi}$ should be much smaller than the typical distance $\hbar v_x/d$ between the levels, implying that the contact is almost ballistic with a transparency close to unity, $1-\mathcal{T}\ll 1$. Second, the applied voltage should be small $\hbar\omega_J\ll\hbar v_x/d$ such that it cannot excite transitions between levels far from the avoided crossings.

The scheme of the levels as functions of $\phi=\omega_J t$ is shown in Fig. 2. Particles captured on the outermost levels at different instants of time $t_k=2\pi k/\omega_J$ were initially in equilibrium with the heat bath and thus are not correlated with each other. Nevertheless, each individual particle performs a series of LZ transitions which might be correlated in principle. However, the phase coherence between the consecutive LZ

events of each particle is lost due to the low-voltage condition, $\omega_J\ll v_x/d$. Indeed, let us consider the trajectories of levels n and $n-1$ between the two crossing points at $\phi=0$ and $\phi=2\pi$. The phases accumulated by the wave function during the time evolutions along the upper- and lower-level trajectories differ from each other by a large amount,

$$\frac{1}{\hbar} \int (\epsilon_n - \epsilon_{n-1}) dt = \frac{1}{\hbar\omega_J} \int_0^{2\pi} (\epsilon_n - \epsilon_{n-1}) d\phi \sim \frac{v_x}{\omega_J d} \gg 1.$$

This allows us to consider the LZ transitions of each particle as independent and to describe the population of levels in terms of LZ probabilities. We assume that the interlevel transitions at $\phi=2\pi k$ and $\phi=\pi+2\pi k$ have tunneling probabilities p_0 and p_π , respectively, which are independent of energy. We will see later that the assumption of constant probabilities is well justified.

We denote the points $\phi=2\pi k$ before and after the transition events as 0^\mp , respectively, while the points $\phi=\pi+2\pi k$ before and after the transitions are denoted as π^\mp . All the respective points 0^+ or 0^- on a level n are equivalent due to the 2π periodicity, so are all the points π^+ or π^- . The transitions illustrated in Fig. 2 impose the relations

$$f_n^+(0^+) = p_0 f_{n-1}^+(0^-) + (1-p_0) f_n^-(0^-), \quad (6)$$

$$f_n^-(\pi^+) = p_\pi f_{n+1}^-(\pi^-) + (1-p_\pi) f_n^+(\pi^-), \quad (7)$$

$$f_{n+1}^-(0^+) = p_0 f_{n+2}^-(0^-) + (1-p_0) f_{n+1}^+(\pi^-), \quad (8)$$

$$f_{n+1}^+(\pi^+) = p_\pi f_n^+(\pi^-) + (1-p_\pi) f_{n+1}^-(\pi^-), \quad (9)$$

on the values of the distribution function f_n before and after the transitions. Here, we introduce the upper + (or -) indices to indicate explicitly the distributions at the spectrum branches increasing (or decreasing) as functions of ϕ . Index n labels the levels consecutively from the lowermost level at $\epsilon=-|\Delta|$ up to the uppermost level at $\epsilon=+|\Delta|$.

Within the model of incoherent LZ transitions, it is appropriate to assume that, between the LZ transition events, the distribution function relaxes according to

$$\frac{\partial f_n}{\partial t} = -\frac{f_n - f_n^{(0)}}{\tau}.$$

Here, τ is a (constant) inelastic relaxation time, which we assume long such that $v_x\tau\gg d$. We denote $f_n=1-2n_\epsilon$, where n_ϵ is the occupation number of a level with an energy ϵ_n , and $f_n^{(0)}=1-2n_\epsilon^{(0)}=\tanh(\epsilon_n/2T)$ is the equilibrium distribution at a given temperature. We will consider low temperatures $T\ll\hbar v_x/d$ such that

$$f_n^{(0)} = \text{sign}(\epsilon_n). \quad (10)$$

Since the superconducting phase difference depends linearly on time the distribution function can be written as $f_n(\phi)=f_n^{(0)}+\tilde{f}_n(\phi)$, where

$$\tilde{f}_n^\pm(\phi) = \begin{cases} \psi_n^\pm \exp(-\hbar\phi/2eV\tau), & 0 < \phi < \pi, \\ \chi_n^\pm \exp[-\hbar(\phi - \pi)/2eV\tau], & \pi < \phi < 2\pi. \end{cases} \quad (11)$$

Using the evolution equation [Eq. (11)], we couple the distribution functions at the consecutive instants of the tunneling events,

$$f_n^\pm(\pi+) = f_n^{(0)} + \chi_n^\pm, \quad f_n^\pm(0-) = f_n^{(0)} + \chi_n^\pm e^{-\nu},$$

$$f_n^\pm(0+) = f_n^{(0)} + \psi_n^\pm, \quad f_n^\pm(\pi-) = f_n^{(0)} + \psi_n^\pm e^{-\nu},$$

where $\nu = \pi\hbar/2eV\tau$. Equations (6)–(9) become

$$\psi_n^+ = p_0[f_n^{(0)} - f_{n-1}^{(0)}] + [p_0\chi_{n-1}^+ + (1-p_0)\chi_n^-]e^{-\nu}, \quad (12)$$

$$\psi_{n+1}^- = p_0[f_{n+2}^{(0)} - f_{n+1}^{(0)}] + [p_0\chi_{n+2}^- + (1-p_0)\chi_{n+1}^+]e^{-\nu}, \quad (13)$$

and

$$\chi_n^- = p_\pi[f_{n+1}^{(0)} - f_n^{(0)}] + [p_\pi\psi_{n+1}^- + (1-p_\pi)\psi_n^+]e^{-\nu}, \quad (14)$$

$$\chi_{n+1}^+ = p_\pi[f_n^{(0)} - f_{n+1}^{(0)}] + [p_\pi\psi_n^+ + (1-p_\pi)\psi_{n+1}^-]e^{-\nu}. \quad (15)$$

According to our picture of the spectral flow through the Andreev levels, the boundary conditions are imposed at the continuum edges in such a way that, for the levels increasing as functions of ϕ , the distribution f_n^+ coincides with the equilibrium at $\epsilon = -|\Delta|$, while, for decreasing levels, the distribution f_n^- coincides with the equilibrium at $\epsilon = +|\Delta|$. Since the bias voltage is low, $eV \ll \hbar v_x/d$, the equilibrium function in both superconducting electrodes can be taken as $f_n^{(0)} = \tanh(\epsilon_n/2T)$. Let us assume that trapping of particles from the continuum occurs at $\phi=0$; the boundary conditions are then formulated for the function ψ_n^+ at $\epsilon = -|\Delta|$ and for ψ_n^- at $\epsilon = +|\Delta|$,

$$\psi_{\epsilon=-|\Delta|}^+ = 0, \quad \psi_{\epsilon=+|\Delta|}^- = 0. \quad (16)$$

In this case, it is convenient to exclude the functions χ using Eqs. (14) and (15) and solve Eqs. (12) and (13) for the functions ψ .

We choose the level index n in such a way that $\epsilon_n > 0$ for $n \geq 1$ and $\epsilon_n < 0$ for $n \leq 0$. Equations (12) and (13) then couple the levels n and $n \pm 2$. Since the temperature is low and the distribution is given by Eq. (10), the right-hand side of these equations vanish for all $n \neq 0, 2$, and the coefficients for $n \geq 2$ and $n \leq 0$ satisfy the homogeneous equations. We assume that there are $N+1$ levels with positive energies and $N+1$ levels with negative energies such that the outermost levels touch the continuum. Therefore, for the uppermost level $n=N+1$, the solution of Eqs. (12) and (13) satisfies the condition $\psi_{N+1}^- = 0$. Similarly, for the lowermost level $n=-N$ the solution satisfies $\psi_{-N}^+ = 0$. We find for $n \geq 2$

$$\psi_n^+ = c^>[e^{-r(N-n+1)}w_- - e^{r(N-n+1)}w_+],$$

$$\psi_n^- = c^<[e^{-r(N-n+1)} - e^{r(N-n+1)}], \quad (17)$$

where

$$w_\pm = \frac{p_0 e^{\pm r} + p_\pi e^{\mp r} - 2p_0 p_\pi \cosh(r)}{\zeta + p_0 p_\pi (1 - e^{\pm 2r}) + p_0 + p_\pi - 2p_0 p_\pi}.$$

The solutions for $n \leq 0$ have the form

$$\psi_n^+ = c^<[e^{r(N+n)} - e^{-r(N+n)}],$$

$$\psi_n^- = c^<[e^{r(N+n)}w_+ - e^{-r(N+n)}w_-]. \quad (18)$$

The effective relaxation rate $r > 0$ is found from the determinant condition $w_+ w_- = 1$ which gives

$$4p_0 p_\pi (\zeta + 1) \sinh^2(r) = (\zeta + p_0 + p_\pi - 2p_0 p_\pi)^2 - (p_0 + p_\pi - 2p_0 p_\pi)^2, \quad (19)$$

where $\zeta = e^{2\nu} - 1$.

For an ideally transparent contact $p_0 = p_\pi = 1$, we find $r = \nu$. For strong relaxation, $\nu \gg 1$, we also have $r \approx \nu$, and the distribution relaxes quickly. The most interesting limit for a general case $p_0, p_\pi \neq 1$ is when inelastic relaxation is weak, $\nu \ll 1$. We find in this limit

$$\sinh^2(r) = \nu(\nu + p_0 + p_\pi - 2p_0 p_\pi) / p_0 p_\pi. \quad (20)$$

The relaxation rate r can be either large or small depending on the probabilities. The inverse rate r^{-1} describes the broadening of distribution over the energy states and plays the role of an effective temperature $T_{\text{eff}} = r^{-1}(d\epsilon/dn) = \pi\hbar v_x/2rd$. The effective temperature can be much higher than the interlevel spacing if $r \ll 1$.

The coefficients $c^>$ and $c^<$ are coupled through the solutions of four nonhomogeneous equations resulting from two equations [Eqs. (12) and (13)] taken for two values $n=2$ and $n=0$. Inspecting equations for other n , we see that only the two coefficients $\psi_0^>$ and ψ_1^- cannot be described by Eqs. (17) and (18) of the homogeneous equations. We write

$$\psi_1^- = \psi_1^{>} + \delta_1^>, \quad \psi_1^- = \psi_1^{<} + \delta_1^{<}, \quad (21)$$

$$\psi_0^+ = \psi_0^{>} + \delta_0^>, \quad \psi_0^+ = \psi_0^{<} + \delta_0^{<}. \quad (22)$$

Here, $\delta_{0,1}^>$ and $\delta_{0,1}^{<}$ are four new unknown coefficients. The coefficients $\psi_1^{>}$ and $\psi_0^{>}$ are defined to satisfy the homogeneous equations for $\epsilon_n > 0$ and are given by Eq. (17); the coefficients $\psi_1^{<}$ and $\psi_0^{<}$ satisfy the homogeneous equations for $\epsilon_n < 0$ and are given by Eq. (18). Inserting Eqs. (21) and (22) into the four equations obtained for $n=2$ and $n=0$ from Eqs. (12) and (13), we find all the four coefficients δ . The result is $\psi_1^- = \psi_1^{>}$ and $\psi_0^+ = \psi_0^{<}$, while

$$\psi_1^{<} - \psi_1^{>} = e^\nu (f_1^{(0)} - f_0^{(0)}), \quad (23)$$

$$\psi_0^{<} - \psi_0^{>} = e^\nu (f_1^{(0)} - f_0^{(0)}). \quad (24)$$

These two equations yield $c^> = c^< = C$, where

$$C[e^{rN}(1 + e^r w_+) - e^{-rN}(1 + e^{-r} w_-)] = 2e^\nu. \quad (25)$$

We set $f_1^{(0)} - f_0^{(0)} = 2$ for low temperatures. Therefore, the distribution possesses the symmetry $\psi_{-n}^+ = -\psi_{n+1}^-$, which is equivalent to the absence of an even-in- ϵ component of the distribution function, $1 - n_{\epsilon - n_{-\epsilon}} = 0$. This implies, in particular, that the shift of the chemical potential of excitations is negligible for low voltages.

IV. CURRENT

The contribution to the current due to the deviation from equilibrium is

$$I_{\text{neq}} = -\frac{2e}{\hbar} \sum_{\epsilon_n > 0} \frac{\partial \epsilon_n}{\partial \phi} \tilde{f}_n, \quad (26)$$

where $\tilde{f}_n = f_n - f_n^{(0)}$. The sum runs only over the localized Andreev states because the continuum states relax quickly so that their distribution is almost in equilibrium. The equilibrium supercurrent has been calculated in Ref. 16 (see also Ref. 1 for a review); it is an oscillating function of the phase difference and thus has no contribution to the dc component.

Denote $\partial \epsilon_n^{\pm} / \partial \phi$ increasing (decreasing) parts of the spectrum $\epsilon_n(\phi)$ as a function of ϕ . We have for the current averaged in time

$$\bar{I} = -\frac{e}{\pi \hbar} \sum_{l=0}^{N/2} \left[\int_0^{\pi} \left(\frac{\partial \epsilon_{n+1}^+}{\partial \phi} \tilde{f}_{n+1}^+ + \frac{\partial \epsilon_n^-}{\partial \phi} \tilde{f}_n^- \right) d\phi + \int_{\pi}^{2\pi} \left(\frac{\partial \epsilon_{n+1}^-}{\partial \phi} \tilde{f}_{n+1}^- + \frac{\partial \epsilon_n^+}{\partial \phi} \tilde{f}_n^+ \right) d\phi \right]_{n=2l+1}. \quad (27)$$

The sum over l runs from 0 to $L=N/2$, where

$$N = 2d\Delta / \pi \hbar v_x$$

is the total number of levels with $\epsilon_n > 0$, including both signs in Eq. (4).

In Eq. (27) we can use the ballistic spectrum with $\mathcal{T} \rightarrow 1$. In this limit $|S_N| = 0$, $|S_A| = 1$, thus the spectrum in Eq. (3) takes the form

$$\cos(\phi/2) = \pm \sin(\beta + \gamma).$$

Calculating the energy derivative of this equation for long junctions $d|\Delta| \gg \hbar v_x$, we find

$$\frac{\partial \epsilon_n^{\pm}}{\partial \phi} = \pm \frac{\hbar v_x}{2d}.$$

We neglected $\partial \gamma / \partial \epsilon$ compared to $\partial \beta / \partial \epsilon$ which holds for all energy levels excluding those in a narrow region near the gap edge, $1 - |\epsilon|/|\Delta| \ll (\hbar v_x / d|\Delta|)^2$. This means, in fact, that neglecting this narrow region, we can use Eqs. (4) and (5) with $\mathcal{T} = 1$ for all n . Using Eq. (11), we obtain for $\nu \ll 1$

$$\bar{I} = \frac{e v_x}{2d} \Phi(p_0, p_{\pi}) = \frac{\pi \hbar v_x}{2e R_0 d} \Phi(p_0, p_{\pi}), \quad (28)$$

where $R_0^{-1} = e^2 / \pi \hbar$ is the quantum of conductance, and

$$\Phi(p_0, p_{\pi}) = -\sum_{l=0}^{N/2} [(\psi_{n+1}^+ - \psi_n^-) + (\chi_n^+ - \chi_{n+1}^-)]_{n=2l+1}.$$

Consider the limit of low relaxation $r \ll 1$ provided $Nr \gg 1$. The limit $r \ll 1$ is realized when $\nu \ll p_0, p_{\pi}$. In this case, Eqs. (15), (17), and (25), give

$$(\psi_{n+1}^+ - \psi_n^-) + (\chi_n^+ - \chi_{n+1}^-) = -\frac{4\nu}{r} e^{-m}. \quad (29)$$

We have from Eq. (29)

$$\Phi(p_0, p_{\pi}) = \frac{4\nu}{r} \sum_{k=0}^{N/2} e^{-r(2k+1)} = \frac{2p_0 p_{\pi}}{p_0 + p_{\pi} - 2p_0 p_{\pi} + \nu}. \quad (30)$$

We keep ν in the denominator since the combination $p_0 + p_{\pi} - 2p_0 p_{\pi}$ vanishes when $p_0, p_{\pi} \rightarrow 1$.

When the inelastic relaxation rate is so small that $N\nu \ll 1$ the effective relaxation r can decrease such that $Nr \ll 1$. Since the product $N(p_0 + p_{\pi} - 2p_0 p_{\pi})$ is generally not small, we find from Eqs. (14), (15), (17), and (25)

$$(\psi_{n+1}^+ - \psi_n^-) + (\chi_n^+ - \chi_{n+1}^-) = -\frac{4p_0 p_{\pi}}{N(p_0 + p_{\pi} - 2p_0 p_{\pi}) + 1},$$

and

$$\Phi(p_0, p_{\pi}) = \frac{2p_0 p_{\pi}}{(p_0 + p_{\pi} - 2p_0 p_{\pi}) + 1/N}. \quad (31)$$

Equations (30) and (31) go one into another for $N \sim 1/\nu$. The exact expression for Φ is found from Eqs. (14), (15), (17), and (25). However, to see the overall behavior of the function $\Phi(p_0, p_{\pi})$, one can approximate it by an interpolation between Eqs. (30) and (31) in the form

$$\Phi(p_0, p_{\pi}) = \frac{2p_0 p_{\pi}}{(p_0 + p_{\pi} - 2p_0 p_{\pi}) + 2\beta}, \quad (32)$$

where $2\beta \approx \max(\nu, N^{-1}) \approx \nu + N^{-1}$.

The probability of LZ tunneling can be easily calculated for the spectrum in the form of Eqs. (4) and (5) if $(1 - \mathcal{T}) \ll 1$. The phase difference is $\phi = \omega_J t + \phi_0$. As a function of time, the distance between two neighboring levels for ϕ close to π is

$$\delta \epsilon = \frac{\hbar v_x \mathcal{T} \omega_J}{d} \sqrt{t^2 + \tau_0^2},$$

where t is small and

$$\tau_0^2 = 4 \sin^2 \alpha' (1 - \mathcal{T}^2) / \mathcal{T}^2 \omega_J^2.$$

Probability of LZ tunneling is

$$p_{\pi} = \exp \left[-\frac{2}{\hbar} \text{Im} \left(\int_0^{i\tau_0} \delta \epsilon dt \right) \right] = \exp \left[-\frac{\omega_0}{\omega_J} \sin^2 \alpha' \right],$$

where

$$\omega_0 = \pi v_x (1 - \mathcal{T}^2) / \mathcal{T} d.$$

The distance between two levels for ϕ close to $\phi=0$ and the corresponding probability of LZ tunneling p_0 are given by the same expressions where $\sin \alpha'$ is replaced with $\cos \alpha'$.

In Eq. (32) the term with β is only important when p_0 and p_{π} are close to unity. Therefore, one can write

$$\Phi(p_0, p_{\pi}) = \left\{ \exp \left[\frac{\omega_0}{\omega_J} \right] \cosh \left[\frac{\omega_0}{\omega_J} \cos(2\alpha') \right] - 1 + \beta \right\}^{-1}. \quad (33)$$

When the bias voltage is low $\omega_J / \omega_0 \ll 1$, such that $\nu \ll p_0, p_{\pi} \ll 1$, we have

$$\Phi(p_0, p_\pi) = 2 \exp\left(-\frac{\omega_0}{\omega_J} [1 + |\cos(2\alpha')|]\right). \quad (34)$$

The low-voltage part is exponential due to small LZ probabilities. The exponent exhibits strong oscillations as a function of α' which can be manipulated by varying the gate voltage.

For higher bias voltages, $\omega_J/\omega_0 \gg 1$, we have $p_0, p_\pi \rightarrow 1$ and

$$\Phi(p_0, p_\pi) = \frac{\omega_J}{\omega_0 + \omega_J \beta} \approx \frac{\omega_J}{\omega_0 + \pi/2\tau + \omega_J/2N}. \quad (35)$$

For these voltages we have two regimes. The I - V curve is linear $I = V/R$ as long as $eV \ll N(\hbar\omega_0 + \pi\hbar/\tau)$. The effective conductance is

$$\frac{1}{R} = \frac{1}{R_0} \frac{\pi v_x d}{\omega_0 + \pi/2\tau}.$$

Inelastic relaxation can be neglected if $\omega_0 \gg \pi/2\tau$. In this case, the conductance is much larger than the conductance quantum $R_0/R = (1 - \mathcal{T}^2)^{-1}$. It is interesting to note that the effective conductance is independent of the gate voltage: it contains the sum of two functions in the exponents for p_0 and p_π , i.e., $(\omega_0/\omega_J)\cos^2 \alpha'$ and $(\omega_0/\omega_J)\sin^2 \alpha'$, which obviously is independent of α' .

With increasing voltage up to $eV \gtrsim N(\hbar\omega_0 + \pi\hbar/\tau)$ but still $eV \ll \hbar v_x/d$, the I - V curve saturates at the value

$$I = Ne v_x d = 2e|\Delta|/\pi\hbar,$$

which is by a factor $N \gg 1$ larger than the critical Josephson current of the junction,¹⁶ $I_c \sim e v_x/d$. Such enhancement of the dc component is characteristic only for long junctions due to a large number of Andreev levels involved into the charge transport. This regime can be realized if the number of levels satisfies $N\omega_0 \ll v_x/d$ or $N(1 - \mathcal{T}) \ll 1$.

For a fully ballistic contact with $p_0 = p_\pi = 1$, i.e., $\omega_0 = 0$, Eq. (35) agrees qualitatively with Refs. 3 and 17. In such an ideal case, a linear part of the I - V curve has an effective conductance proportional to the inelastic mean free time; it disappears when $\tau \rightarrow \infty$ while the plateau region starts from zero voltage. Our results show, however, that in any realistic junction, the linear part in the I - V curve can exist even for

$\tau \rightarrow \infty$. In this limit, both the effective conductance and the onset of the saturated-current regime are controlled by the contact transparency.

V. CONCLUSIONS

To summarize, we have considered the charge transport in a nearly ballistic single-mode SINIS junction with a length d longer than the superconducting coherence length ξ and a contact transparency close to unity. In this junction, the energy spectrum of Andreev states has a large number of levels separated from each other by small minigaps which do not vanish in a realistic case when the transmission is not exactly unity. We focus on temperatures much lower than the typical distance between the Andreev levels assuming a slow rate of inelastic relaxation. In the limit of low bias voltages such that the Josephson frequency is smaller than the typical interlevel distance, we have derived and solved the kinetic equation for the quasiparticle distribution on the Andreev levels that takes into account both inelastic relaxation and voltage-driven LZ transitions between the levels. We have shown that the LZ transitions enhance the action of each other and lead to a drastic increase of the dc current. Its voltage dependence is first exponential due to small probabilities of LZ tunneling. Next, it goes over into a linear relation with a slope determined by the minigaps in the spectrum. At yet higher voltages (which are still much lower than the interlevel distance) when the LZ probabilities approach unity, the dc saturates at a value far exceeding the critical Josephson current of the junction. Single-mode SINIS junctions made of carbon nanotubes or semiconductor nanowires with $d \sim 500$ nm and aluminum-based superconductor leads described so far in the literature^{11,12} have $\hbar v_x/d \sim 3.5$ meV and $\Delta \sim 0.25$ meV and do not satisfy the condition of long junctions. One expects, however, that the long-junction requirements could be fulfilled using lead materials with higher T_c and employing nanowires with lower $\hbar v_x/d$. The temperatures of interest would then be in a 100 mK range.

ACKNOWLEDGMENTS

We are grateful to Yu. Galperin, A. Mel'nikov, and V. Shumeiko for stimulating discussions. This work was supported by the Academy of Finland (Grant No. 213496, Finnish Programme for Centres of Excellence in Research 2002–2007/2006–2011) and by the Russian Foundation for Basic Research Grant No. 06-02-16002-a.

¹A. A. Golubov, M. Yu. Kupriyanov, and E. Il'ichev, Rev. Mod. Phys. **76**, 411 (2004).

²A. F. Andreev, Zh. Eksp. Teor. Fiz. **46**, 1823 (1964) [Sov. Phys. JETP **49**, 924 (1964)].

³U. Gunsenheimer and A. D. Zaikin, Phys. Rev. B **50**, 6317 (1994).

⁴D. Averin and A. Bardas, Phys. Rev. Lett. **75**, 1831 (1995).

⁵D. Averin and A. Bardas, Phys. Rev. B **53**, R1705 (1996).

⁶G. E. Blonder, M. Tinkham, and T. M. Klapwijk, Phys. Rev. B

25, 4515 (1982).

⁷M. Octavio, M. Tinkham, G. E. Blonder, and T. M. Klapwijk, Phys. Rev. B **27**, 6739 (1983).

⁸E. N. Bratus', V. S. Shumeiko, and G. Wendin, Phys. Rev. Lett. **74**, 2110 (1995).

⁹N. B. Kopnin and V. M. Vinokur, Europhys. Lett. **61**, 824 (2003).

¹⁰E. N. Bratus', V. S. Shumeiko, E. V. Bezuglyi, and G. Wendin, Phys. Rev. B **55**, 12666 (1997).

¹¹M. R. Buitelaar, W. Belzig, T. Nussbaumer, B. Babic, C. Bruder,

- and C. Schonenberger, Phys. Rev. Lett. **91**, 057005 (2003); A. Kasumov, M. Kociak, M. Ferrier, R. Deblock, S. Gueron, B. Reulet, I. Khodos, O. Stephan, and H. Bouchiat, Phys. Rev. B **68**, 214521 (2003); P. Jarillo-Herrero, J. A. van Dam, and L. P. Kouwenhoven, Nature (London) **439**, 953 (2006).
- ¹²Y. J. Doh, J. A. van Dam, A. L. Roest *et al.*, Science **309**, 272 (2005).
- ¹³N. B. Kopnin, A. S. Mel'nikov, and V. M. Vinokur, Phys. Rev. Lett. **96**, 146802 (2006).
- ¹⁴C. W. J. Beenakker, Phys. Rev. Lett. **67**, 3836 (1991).
- ¹⁵U. Schüssler and R. Kümmel, Phys. Rev. B **47**, 2754 (1993); G. A. Gogadze and A. M. Kosevich, Fiz. Nizk. Temp. **24**, 716 (1998) [Low Temp. Phys. **24**, 540 (1998)]; P. Samuelsson, J. Lantz, V. S. Shumeiko, and G. Wendin, Phys. Rev. B **62**, 1319 (2000); D. D. Kuhn, N. M. Chtchelkatchev, G. B. Lesovik, and G. Blatter, *ibid.* **63**, 054520 (2001); A. Jacobs and R. Kümmel, *ibid.* **71**, 184504 (2005).
- ¹⁶A. V. Galaktionov and A. D. Zaikin, Phys. Rev. B **65**, 184507 (2002).
- ¹⁷A. Ingerman, G. Johansson, V. S. Shumeiko, and G. Wendin, Phys. Rev. B **64**, 144504 (2001).